

Superconducting phase sequence in R_xC_{60} fullerides ($R=Sm$ and Yb)

Misaho Akada,¹ Toshinari Hirai,² Junji Takeuchi,² Takao Yamamoto,¹ Ryotaro Kumashiro,¹ and Katsumi Tanigaki¹

¹*Department of Physics, Graduate School of Science, Tohoku University and CREST-JST, 6-3 Aoba Aramaki Aoba-ku, Sendai, Miyagi 980-8578, Japan*

²*Department of Materials Science, Graduate School of Science, Osaka City University and CREST-JST, 3-3-138 Sugimoto, Sumiyoshi, Osaka 558-8585, Japan*

(Received 1 November 2005; published 17 March 2006)

The true superconducting phase in rare-earth C_{60} fullerides R_xC_{60} ($R=Yb$ and Sm) is not $R_{2.75}C_{60}$ previously reported. Moreover, no superconductivity is observed in $Sm-C_{60}$ fullerides. The phase sequence between $Yb-C_{60}$ fullerides and $Sm-C_{60}$ ones as a function of the intercalant concentration of x is shown to be greatly different, although Yb and Sm are the same family of rare-earth elements with the divalent valence state. This can explain the loss of superconductivity in Sm_xC_{60} and suggests the true superconducting phase. The whole picture of rare-earth C_{60} fullerides is described.

DOI: 10.1103/PhysRevB.73.094509

PACS number(s): 74.70.Wz

I. INTRODUCTION

The doped C_{60} 's with a half-filling band, identical to the trivalent state of C_{60} , are metallic and superconducting, and no superconductivity is observed in the other filling in the t_{1u} associated C_{60} fullerides.¹⁻³ Such features have been exemplified for alkali metal doped C_{60} fullerides.⁴ In contrast, the t_{1g} band-associated C_{60} fullerides show a different situation. Alkaline-earth metal ($Ae=Sr$ and Ba) doped C_{60} fullerides show superconductivity when they are in the body-centered orthorhombic phase (bco) with the stoichiometry of Ae_4C_{60} .⁵⁻⁸ The change in properties upon the odd-even stoichiometries observed in the t_{1u} associated fullerides (see a simplified situation in the t_{1u} C_{60} fullerides shown in Fig. 1) is no longer observed in these t_{1g} associated ones.⁹

The rare-earth metal doped C_{60} fullerides were also reported to show superconductivity with a very different crystal phase of $R_{2.75}C_{60}$'s ($R=Yb$ and Sm) with superlattice structure.^{10,11} This had been believed to be the true superconducting phase for a long time after the publications. This assignment, however, seems to be unreasonable since the divalent state of R intercalants gives rise to a band filling in the vicinity of the t_{1u} upper band edge as seen in Fig. 1 and this is a very different situation encountered for the other t_{1g} C_{60} fullerides made from Sr and Ba (Refs. 5–8 and 12) and their mixtures with K and Rb .⁹ In view of the fundamental knowledge so far achieved from the electronic states of alkali and alkaline-earth metal doped C_{60} 's as described above, such a situation cannot be expected and had to be clarified. If this was indeed the true case, the theories so far proposed had to be modified. In the late 1990s, we have clearly shown that $R_{2.75}C_{60}$ fullerides ($R=Yb$ and Sm) are not the true superconducting phases, even though the experimental fact that the superconductivity can be observed in $Yb-C_{60}$ fullerides¹⁰ is correct. Moreover, we have pointed out that any superconductivity cannot be observed in the case of $Sm-C_{60}$ fullerides,¹³ even though the superconductivity was reported in the literature.¹¹

At that time, however, the real superconducting phase in the $Yb-C_{60}$ fullerides as well as the reason why the superconductivity cannot be observed in the $Sm-C_{60}$ ones has not

fully been understood.^{13,14} This paper elucidates that the phase sequence of C_{60} fullerides is very much different between Yb and Sm fullerides, although both of the elements are the same family of divalent rare-earth metals. This will give the true whole scenario of what occurs in the rare-earth C_{60} fullerides.

II. EXPERIMENT

$R_{2.75}C_{60}$ ($R=Yb$ and Sm) fullerides were prepared from the direct reactions of C_{60} and Yb or Sm metals with different stoichiometries. C_{60} commercially available from the TERM company was mixed with rare-earth metals and introduced to a tantalum cell encapsulated by a quartz tube. The mixed samples were pelletized at room temperature and then heated at 873 K for about 10 h. The preheated samples were ground after being taken out of the glass tubes in a glove box and again heated at 923 K for 24–72 h. The resulting fullerides were subjected to the magnetic measurements using a Quantum Design MPMS7 apparatus for checking superconductivity and their structure was studied by x-ray diffraction measurements carried out by high-energy synchrotron radiation at BL02B2 of SPring-8.

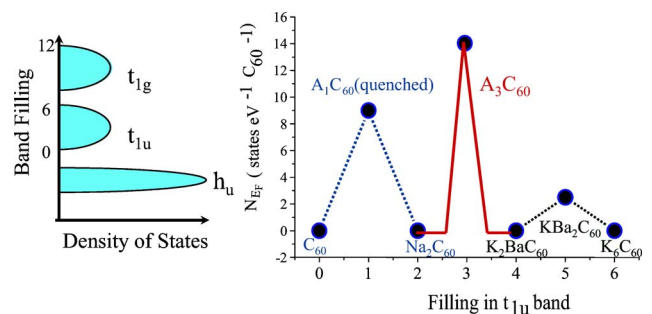


FIG. 1. (Color online) The variation of N_{E_F} as a function of band filling in the t_{1u} associated C_{60} fullerides. The picture depicted shown in the left is a simplified band picture.

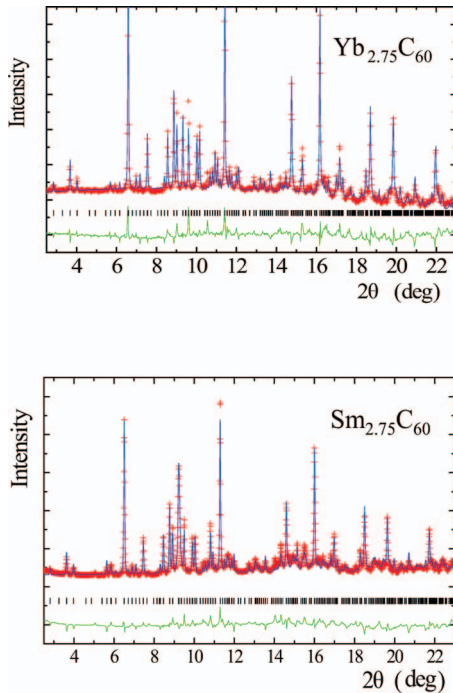


FIG. 2. (Color) X-ray diffraction patterns of $\text{Yb}_{2.75}\text{C}_{60}$ and $\text{Sm}_{2.75}\text{C}_{60}$ collected with synchrotron radiation. Rietveld fittings are included in the figure.

III. RESULTS AND DISCUSSION

A. Nonsuperconductivity in $R_{2.75}\text{C}_{60}$ ($R=\text{Yb}$ and Sm)

The C_{60} fulleride with the nominal stoichiometry $\text{Yb}_{2.75}\text{C}_{60}$, being reported to be superconducting, was successfully prepared from the pelletized C_{60} mixed with Yb by heating treatments. Figure 2 (upper) shows the Rietveld analysis using the structural parameters reported previously.¹⁰ All the observed peaks including low angle peaks associated with the superlattice structure were well indexed. The superlattice structure can be created by the ordered deficiency of Yb, caused by the strain due to the small ionic radius of the divalent Yb and this is in good agreement with the literature.¹⁰ The refinement parameters are $a=2.7772$, $b=2.7716$, and $c=2.7715$ in the space group of $Pcab$ (No. 61, option2) with $R_p=3.00$ and $R_w=4.23$. Therefore it is evident that the $\text{Yb}_{2.75}\text{C}_{60}$ phase made in the present study is the same crystal phase that has previously been reported.

We have tried to prepare Yb- C_{60} fullerides by changing the nominal stoichiometries ranging from 1 to 6 per C_{60} . When the concentration of Yb is less than 2.75, no other stable crystal phases were detected, and a phase separation between pristine C_{60} and $\text{Yb}_{2.75}\text{C}_{60}$ was observed. When the Yb amount was increased larger than three, some other phases formed and the peak intensities indexed to be those of $\text{Yb}_{2.75}\text{C}_{60}$ were reduced.

When Sm was used as an intercalant, the same crystal phase reported to show superconductivity was also able to be made together with a small amount of A15 Sm_3C_{60} . The Rietveld analysis is shown in Fig. 2 (lower). It should be noted that the crystal phase was greatly improved when it is

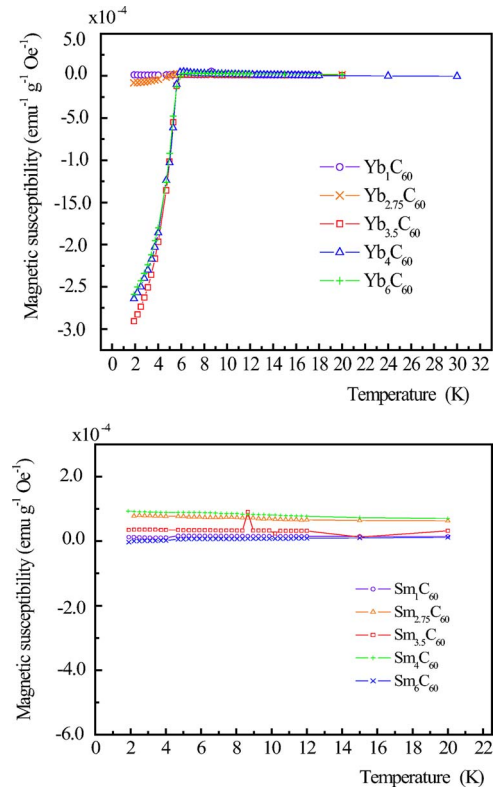


FIG. 3. (Color online) Magnetic moments measured by SQUID under a low magnetic field of 10 Oe for $R_x\text{C}_{60}$ ($R=\text{Yb}$ and Sm).

compared to that reported previously.¹¹ The two-phase Rietveld fitting using 95% $\text{Sm}_{2.75}\text{C}_{60}$ and 5% A15 Sm_3C_{60} has been made and the refined parameters of $a=2.8161$, $b=2.8200$, and $c=2.8169$ nm in the space group of $Pcab$ (No. 61, option2) for $\text{Sm}_{2.75}\text{C}_{60}$ and $a=1.1105$ nm for A15 Sm_3C_{60} were obtained with $R_p=8.26\%$ and $R_w=10.61\%$. Crystallographically no difference was noticed between $\text{Yb}_{2.75}\text{C}_{60}$ and $\text{Sm}_{2.75}\text{C}_{60}$ except for the additional A15 phase.

For confirmation of the superconductivity in $\text{Yb}_{2.75}\text{C}_{60}$, magnetic susceptibility measurements for detecting the su-

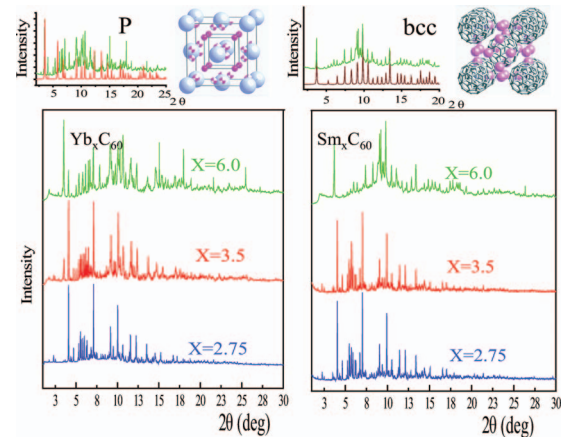


FIG. 4. (Color) The phases appearing in Yb_xC_{60} and Sm_xC_{60} as a function of x . Both systems show different phase sequences as described in the text. The saturation phase in Yb_xC_{60} is in primitive cubic, while the one in Sm_xC_{60} is bcc.

perconducting diamagnetic signals have been carried out using a superconducting quantum interference device (SQUID) under a low-magnetic field of 10 Oe. The measurements showed that any important superconductivity does not appear, except for only a trace amount of superconducting fraction as shown in Fig. 3. Considering the pure crystal phase of $Yb_{2.75}C_{60}$ made in the present experiments, the superconducting fraction was surprisingly only less than 1%. Therefore the observed superconductivity should not be ascribed to the $Yb_{2.75}C_{60}$ phase but ascribed to another coexisting minor crystal phase.

The existence of superconductivity was also checked for $Sm_{2.75}C_{60}$, but surprisingly no symptom of superconductivity was detected. Considering its high crystal quality described earlier, it is evident that the $Sm_{2.75}C_{60}$ fulleride is not superconducting.

In order to have more detailed confirmation, we have measured superconducting magnetic susceptibilities both for Yb_xC_{60} and Sm_xC_{60} fullerides by changing the component ratios of x ranging from 2.75 to 6 in the feed. When $x=4$ is used in Yb_xC_{60} , the superconducting diamagnetic susceptibility was greatly increased. It is also important that the magnetic susceptibility is in turn decreased, when the stoichiometry of $x=6$ in the feed was used. These situations can be clearly seen in Fig. 3. Since, as explained earlier, it is evident that some other crystal phases appear from the x-ray diffraction studies when x is over three, the superconductivity should be ascribed to the crystal phase other than the superlattice $Yb_{2.75}C_{60}$ phase previously reported. All the data presented here clearly display that $Yb_{2.75}C_{60}$, which has so far been believed to be the real superconducting phase, is not the true superconducting phase, but that another phase appearing in Yb_xC_{60} with x larger than three is superconducting. This will be discussed later.

In the case of C_{60} fullerides with Sm intercalants, no superconductivity was detected for all the component ratios of x as seen in Fig. 3. It should be important to note that we did not see any symptom of superconductivity among more than 50 samples in our experiments. This situation is completely different from the previous reports.¹⁵⁻¹⁷ In any event the experiments described in the present paper clearly show that the superconductivity observed in R_xC_{60} 's ($R=Yb$ and Sm) does not stem from the $R_{2.75}C_{60}$ superlattice phase. Furthermore, the physical properties are surprisingly very much differentiated between Yb_xC_{60} and Sm_xC_{60} .

B. Structural sequence in Yb_xC_{60} and Sm_xC_{60}

For the purpose of understanding the differences in physical properties between $Yb-C_{60}$ and $Sm-C_{60}$ fullerides, the structural sequence has been studied. As shown in Fig. 4, both systems give rise to the $R_{2.75}C_{60}$ phase with superlattice structure first. It is important that the famous superconducting crystal phase of fcc A_3C_{60} fullerides ($A=K$ and Rb) does not take place in both systems.^{2,19,20} They show a different structural evolution from each other as a function of intercalant concentration.

The $Yb-C_{60}$ system shows a structural sequence in the primitive cubic lattice. After passing through the first super-

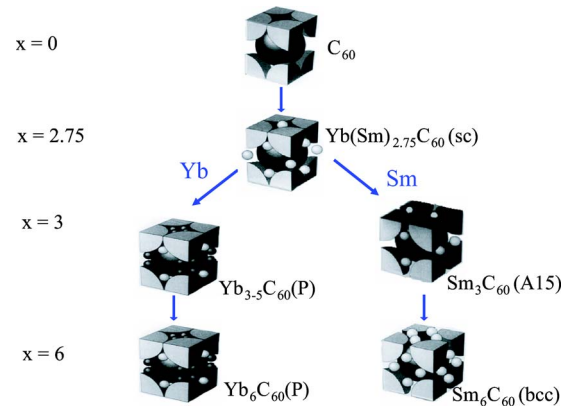


FIG. 5. (Color online) The phase sequence in Yb- and Sm- C_{60} fullerides as a function of dopant concentration.

lattice $Yb_{2.75}C_{60}$ phase, the fullerides approach to Yb_6C_{60} with keeping the primitive cubic cell. The important phases, such as fcc A_3C_{60} ($A=K$ and Rb) and A15 Ae_3C_{60} ($Ae=Sr$ and Ba), are not created. Similar situations have been so far experienced for Na_xC_{60} ,²¹ Ca_xC_{60} ,²² and Li_xCsC_{60} .²³ On the other hand, the structural sequence in Sm_xC_{60} proceeds from $Sm_{2.75}C_{60}$ through A15 Sm_3C_{60} (body-centered cubic (bcc) cell when the C_{60} orientation is ignored) to bcc Sm_6C_{60} . This situation is reminiscent to that experienced for Ba_xC_{60} (in the case of Sr , the fcc Sr_3C_{60} coexists with the A15 phase).^{5,6,8} However, body-centered orthorhombic (bco) type Sm_4C_{60} does not form and this is very different from that in the Ba and $Sr C_{60}$ fulleride systems.¹²

The structural sequence thus determined can be schematically viewed in Fig. 5. In the structural sequence in Yb_xC_{60} , the Yb_xC_{60} with $x=(3+\alpha) \sim 5$ can form. This phase can possibly show superconductivity as a t_{1g} -derived band associated superconductor. Exactly the same situation can be reported for Ca_xC_{60} .²² However, this superconducting phase does not take place in the bcc structural sequence of Sm_xC_{60} . Moreover, even in the bcc sequence, the well-known superconducting bco R_4C_{60} phase is not made. This conclusion can reasonably explain why we do not see any superconductivity in the Sm_xC_{60} fulleride system.

The reason why we do not have the superconducting bco Ae_4C_{60} phase in the bcc structural sequence of Sm_xC_{60} may well be understood when the ionic radii (r^+) are taken into account as displayed in Fig. 6. The r^+ of Sm^{2+} is smaller than that of Sr^{2+} . Therefore it seems that the bco Sm_4C_{60} will be less stable. Actually, no bco phase is reported in the case of the $Eu-C_{60}$ fulleride.²⁴⁻²⁶ The ionic radius of Yb^{2+} is much smaller than that of Sm^{2+} and even close to that of Ca^{2+} . It seems very reasonable that the structural sequence becomes the same between Yb_xC_{60} and Ca_xC_{60} . As a consequence, although Yb and Sm are the same group of divalent rare-earth elements, the structural sequence between Yb_xC_{60} and Sm_xC_{60} becomes dissimilar. In turn, this can explain why very different electronic properties can be observed between Yb and Sm fullerides. This understanding takes a different position from that of the other group,¹⁴ although the experimental fact that the $Sm_{2.75}C_{60}$ does not show any superconductivity becomes a consensus now.

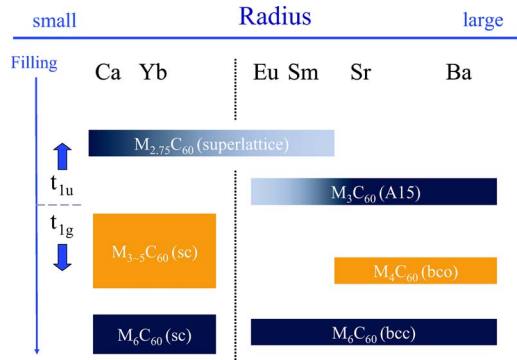


FIG. 6. (Color online) The relationship between the phases and the ionic radii of the dopants in Ae and RC_{60} fullerides. The ionic radii can well explain the crystal phases made in these systems.

C. The true superconducting phase in Yb_xC_{60}

Along with the scenario described earlier, the structural sequence in Yb_xC_{60} is modeled in Fig. 7. Due to the stresses and the strains in the lattice caused by the small r^+ of the divalent Yb^{2+} , the fcc Yb_3C_{60} is no longer stable and one Yb atom from eight in the tetrahedral interstitial sites will be kicked out from the fcc Bravais lattice leaving with the composition of $Yb_{11}(C_{60})_4$. Therefore more stable $Yb_{2.75}C_{60}$ [this stoichiometry comes from $Yb_{11}(C_{60})_4/4$] can form with a superlattice structure having the ordered Yb vacancies as can be clarified by x-ray diffraction analyses. With deviation of intercalants in both tetrahedral and octahedral interstitial sites, more intercalants can interstitially be accommodated in the cell to form Yb_xC_{60} ($x=3+\alpha\sim 5$), until they reach the saturation phases. This structural sequence can end up with full accommodation of the Yb_6C_{60} stoichiometry. The superconductivity can occur in Yb_xC_{60} ($x=3+\alpha\sim 5$) as a t_{1g} -derived band associated superconductor. However, it cannot still be completely ruled out that the superconductivity may relate to the graphite intercalations recently gathering much attractions.¹⁸

So far the primitive cubic cell having the stoichiometry of M_xC_{60} ($3 < x \leq 6$) has been found for Na_xC_{60} , Li_xCsC_{60} , and

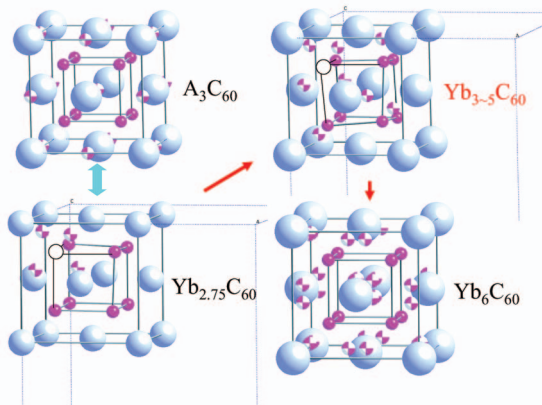


FIG. 7. (Color) The phase sequence of Yb_xC_{60} with x . The primitive cubic cell holds until the saturation phase comes up with increasing x . The superconductivity is considered to occur in $Yb_{3+\alpha}C_{60}$.

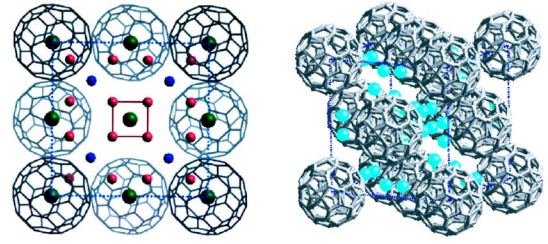


FIG. 8. (Color online) The structure of the M_xC_{60} phase with $x=3-6$ in the primitive cubic cell. The dopants surrounding the octahedral one occupy their positions in a random fashion keeping with the primitive cubic symmetry. The saturation phase is generally M_6C_{60} . In the case of Na, x ranging to 11 is reported (Ref. 27).

Ca_xC_{60} . The structure of the former two fullerides is depicted in Fig. 8. Among these three fullerides, superconductivity has been recognized for the latter two compounds.^{22,23} The missing of superconductivity in Na_xC_{60} may be understood considering the less electron transfer from Na to C_{60} as well as the disordered position of Na in the interstitial sites.

Although the superconducting fraction cannot be zero even in the case of the nominal $Yb_{2.75}C_{60}$ due to the contamination of the true superconducting phase as seen in Fig. 9, we have made a comparison between nonsuperconducting $Yb_{2.75}C_{60}$ and the superconducting $Yb_{3+\alpha}C_{60}$ made from the nominal $Yb_{3.5}C_{60}$, the latter of which shows the highest superconducting fraction in our experiments. Figure 10 shows the magnetic susceptibility χ_{Pauli} observed under high magnetic fields for these two samples. The χ_{Pauli} data were obtained from the subtraction between 4 and 6 T of magnetic fields for excluding the small ferroimpurities generally made in the C_{60} fullerides. Using the equation of $\chi_{\text{Pauli}}=2\mu_B^2N_{E_F}$ where μ_B denotes the Bohr magneton, the density of states at the fermi level N_{E_F} was evaluated to be 9 and 18–30 states $eV^{-1}(C_{60}\text{-mole})^{-1}$ for $Yb_{2.75}C_{60}$ and $Yb_{3+\alpha}C_{60}$, respectively. Apparently N_{E_F} of $Yb_{3+\alpha}C_{60}$ is much larger than that of $Yb_{2.75}C_{60}$. The result is not in disagreement with the occurrence of superconductivity in $Yb_{3+\alpha}C_{60}$, but not in $Yb_{2.75}C_{60}$.

D. The whole picture of the phase sequence in C_{60} fullerides

The whole picture of the phase sequence in C_{60} fullerides is shown in Fig. 11. As is well known, fcc

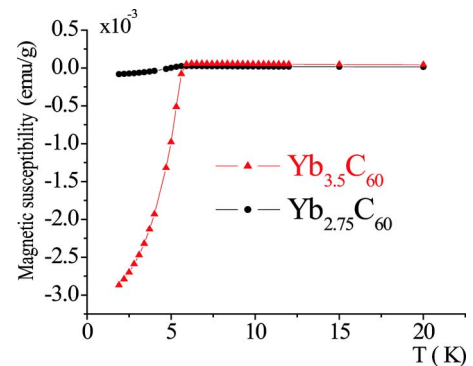


FIG. 9. (Color online) The superconducting diamagnetic susceptibilities of the nonsuperconducting $Yb_{2.75}C_{60}$ and the superconducting $Yb_{3.5}C_{60}$ (here 3.5 is the stoichiometry of Yb in the feed).

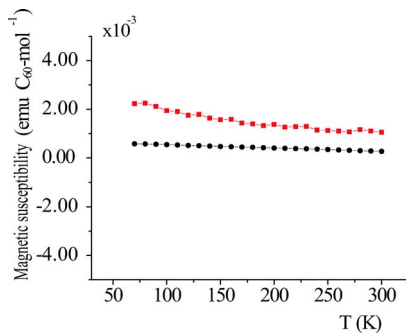


FIG. 10. (Color online) The Pauli magnetic susceptibilities of nonsuperconducting $Yb_{2.75}C_{60}$ (solid circles) and superconducting $Yb_{3.5}C_{60}$ (solid squares).

$C_{60} \rightarrow fcc A_3C_{60} \rightarrow bct A_4C_{60} \rightarrow bcc A_6C_{60}$ occur in the case of alkali metal ($A=K$ and Rb). When alkaline-earth metals ($Ae=Sr$ and Ba) are used, the phase sequence of $fcc C_{60} \rightarrow A15 Ae_3C_{60} \rightarrow bco Ae_4C_{60} \rightarrow bcc Ae_6C_{60}$ takes place. In the case of rare-earth elements ($R=Yb, Sm,$ and Eu), as is described in the present paper, $fcc C_{60} \rightarrow Yb_{2.75}C_{60} \rightarrow$ primitive cubic $Yb_{3+\alpha}C_{60}$ and $fcc C_{60} \rightarrow (Sm, Eu)_{2.75}C_{60} \rightarrow A15 (Sm, Eu)_3C_{60}$ (trace amount) $\rightarrow bcc (Sm, Eu)_6C_{60}$ occur. For Na as an intercalant, $fcc C_{60} \rightarrow fcc Na_2C_{60} \rightarrow [fcc Na_3C_{60}; missing] \rightarrow$ primitive cubic $Na_6C_{60} \rightarrow$ primitive cubic $Na_{11}C_{60}$. In the case of La , La carbides showing superconductivity with $T_c=12$ and 6 K form very fast without making C_{60} fullerenes.²⁸ The superconducting phases are $fcc A_3C_{60}$, $bco Ae_4C_{60}$, primitive cubic $R_{3+\alpha}C_{60}$ in the case of Ca and Yb , although still the possible contribution of graphite intercalations cannot completely be ruled out.¹⁸ No superconducting phases are observed in the case of $Na, Eu,$ and Sm . It is still an open question of whether $fcc/bco Cs_3C_{60}$ is superconducting or not.²⁹

IV. CONCLUSION

Both $Yb_{2.75}C_{60}$ and $Sm_{2.75}C_{60}$ were reexamined and unambiguously confirmed not to be superconducting. The true superconducting phase of $Yb-C_{60}$ fullerenes is most likely in the t_{1g} -derived band. Furthermore, no superconductivity was observed in the case of Sm_xC_{60} . These could be understood by the different phase sequences between $Yb-C_{60}$ and $Sm-C_{60}$ fullerenes. In any case, we have no exceptions in the

Structural sequence of M_xC_{60} fullerenes

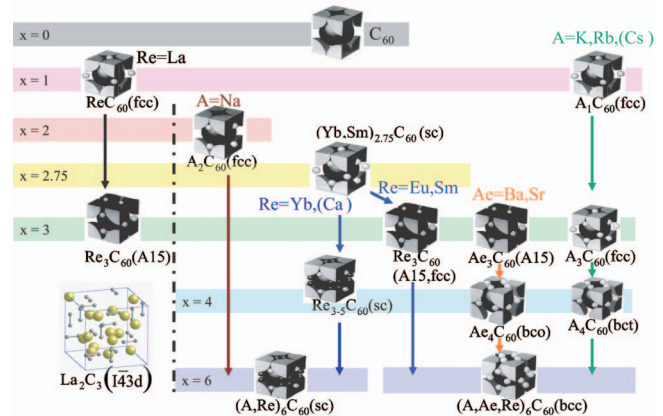


FIG. 11. (Color) The whole picture of the phase sequences made in C_{60} fullerenes.

experimental picture of t_{1u} -associated fullerene superconductors now. The most recent theories,^{30–34} taking into account the cooperative contributions of on-site Coulomb electron-electron repulsion U and electron-phonon interaction V in the framework of the phonon-mediated superconductivity under the dynamic Jahn-Teller distortion of the triply degenerate t_{1u} orbitals of C_{60} , can explain the superconductivity occurring in the t_{1u} -associated fullerenes. The experimental facts do not have to require any modifications to these theories as described in the present paper.

ACKNOWLEDGMENTS

We are grateful to the staff members at SPring8 (beamline BL02B2). The synchrotron radiation experiments were performed by the approval of the Japan Synchrotron Radiation Research Institute (JASRI) as Nanotechnology Support Project. This work was supported by Creation of Nanodevices and Systems Based on New Physical Phenomena and Functional Principles of CREST of JST. The present work is also partially supported by the Tohoku University 21 century COE program “Particle-Matter Hierarchy” of MEXT Japan. This work was performed by a Grant-in-Aid from the Ministry of Education, Culture, Sports, Science, and Technology of Japan, Nos. 13304031 and 17038001.

¹R. C. Haddon, A. F. Hebard, M. J. Rosseinsky *et al.*, Nature (London) **350**, 320 (1991).
²A. F. Hebard, M. J. Rosseinsky, R. C. Haddon, D. W. Murphy, S. H. Glarum, T. T. M. Palstra, A. P. Ramirez, and A. R. Kortan, Nature (London) **350**, 600 (1991).
³K. Tanigaki, I. Hirose, T. W. Ebbesen, J. Mizuki, Y. Shimakawa, Y. Kubo, J. S. Tsai, and S. Kuroshima, Nature (London) **356**, 419 (1992).
⁴K. Tanigaki and K. Prassides, J. Mater. Chem. **5**, 1515 (1995).
⁵A. R. Kortan, N. Kopylov, S. Glarum, E. M. Gyorogy, A. P.

Ramirez, R. M. Fleming, O. Zhou, F. A. Thiel, P. L. Trevor, and R. C. Haddon, Nature (London) **360**, 566 (1992).
⁶M. Baenitz, M. Heinze, K. Luders, H. Werner, R. Schlogl, M. Weiden, G. Sporn, and F. Steglich, Solid State Commun. **96**, 539 (1995).
⁷B. Gogoi, K. Kordatos, H. Suematsu, K. Tanigaki, and K. Prassides, Phys. Rev. B **58**, 1077 (1998).
⁸C. M. Brown, S. Taga, B. Gogoi, K. Kordatos, S. Margadonna, K. Prassides, Y. Iwasa, K. Tanigaki, A. N. Fitch, and P. Pattison, Phys. Rev. Lett. **83**, 2258 (1999).

- ⁹Y. Iwasa, H. Hayashi, T. Furudate, and T. Mitani, *Phys. Rev. B* **54**, 14960 (1996).
- ¹⁰E. Ozdas, A. R. Kortan, N. Kopylov, A. P. Ramirez, T. Siegrist, K. M. Rabe, H. E. Bair, S. Schuppler, and P. H. Citrin, *Nature (London)* **375**, 126 (1995).
- ¹¹X. H. Chen and G. Roth, *Phys. Rev. B* **52**, 15534 (1995).
- ¹²A. R. Kortan, N. Kopylov, E. Ozdas, S. Glarum, A. P. Ramirez, R. M. Fleming, and R. C. Haddon, *Chem. Phys. Lett.* **223**, 501 (1994).
- ¹³J. Takeuchi, K. Tanigaki, and B. Gogia, in *Nanonetwork materials: Fullerenes, Nanotubes and Related Systems*, edited by S. Saito *et al.*, AIP Conf. Proc. No. 590 (AIP, Melville, NY, 2001), pp. 361–364.
- ¹⁴J. Arvanitidis, K. Papagelis, S. Margadonna, K. Prassides, and A. N. Fitch, *Nature (London)* **425**, 599 (2003).
- ¹⁵X. H. Chen, S. Y. Li, G. G. Qian, K. Q. Ruan, and L. Z. Cao, *Phys. Rev. B* **57**, 10770 (1998).
- ¹⁶X. H. Chen, Z. S. Liu, S. Y. Li, D. H. Chi, and Y. Iwasa, *Phys. Rev. B* **60**, 6183 (1999).
- ¹⁷Z. Sun, X. H. Chen, T. Takenobu, and Y. Iwasa, *J. Phys.: Condens. Matter* **12**, 8919 (2000).
- ¹⁸T. Weller, M. Ellerby, S. S. Saxena, R. Smith, and N. Skipper, *Nat. Phys.* **1**, 39 (2005).
- ¹⁹Peter W. Stephens *et al.*, *Nature (London)* **350**, 632 (1991).
- ²⁰M. J. Rosseinsky, A. P. Ramirez, S. H. Glarum, D. W. Murphy, R. C. Haddon, A. F. Hebard, T. T. M. Palstra, A. R. Kortan, S. M. Zahurak, and A. V. Makhija, *Phys. Rev. Lett.* **66**, 2830 (1991).
- ²¹M. J. Rosseinsky, D. M. Murphy, R. M. Fleming, R. Tycko, A. P. Ramirez, T. Siegrist, G. Dabbagh, and S. E. Barrett, *Nature (London)* **356**, 416 (1992).
- ²²A. R. Kortan, N. Kopylov, S. Glarum, E. M. Gyrogy, A. P. Ramirez, R. M. Fleming, F. A. Thiel, P. L. Trevor, and R. C. Haddon, *Nature (London)* **355**, 529 (1992).
- ²³M. Kosaka, K. Tanigaki, K. Prassides, S. Margadonna, A. Lappas, C. M. Brown, and A. N. Fitch, *Phys. Rev. B* **59**, R6628 (1999).
- ²⁴H. Yoshikawa, S. Kuroshima, I. Hirose, K. Tanigaki, and J. Mizuki, *Chem. Phys. Lett.* **239**, 103 (1995).
- ²⁵Y. Ksari-Habiles, D. Claves, G. Chouteau, Ph. Touzain, C. Jean-dey, J. L. Oddou, and A. Stepanov, *J. Phys. Chem. Solids* **58**, 1771 (1997).
- ²⁶D. Claves, Y. Ksari-Habiles, G. Chouteau, and Ph. Touzain, *Solid State Commun.* **106**, 431 (1998).
- ²⁷T. Yildirim, O. Zhou, J. E. Fishcher, N. Bykovetz, R. A. Strongin, M. A. Cichy, A. B. Smith III, C. L. Lin, and R. Jelinek, *Nature (London)* **360**, 568 (1992).
- ²⁸M. Akada, T. Hirai, J. Takeuchi, N. Hiroshima, R. Kumashiro, T. Yamamoto, and K. Tanigaki, *Phys. Rev. B* **72**, 132505 (2005).
- ²⁹S. Fujiki, Y. Kubozono, M. Kobayashi, T. Kambe, Y. Rikiishi, S. Kashino, K. Ishii, H. Suematsu, and A. Fujiwara, *Phys. Rev. B* **65**, 235425 (2002).
- ³⁰O. Gunnarsson, *Rev. Mod. Phys.* **69**, 5754 (1997).
- ³¹S. Suzuki, S. Okada, and K. Nakao, *J. Phys. Soc. Jpn.* **69**, 2615 (2000).
- ³²M. Fabrizio and E. Tosatti, *Phys. Rev. B* **55**, 13465 (1997).
- ³³J. E. Han, O. Gunnarsson, and V. H. Crespi, *Phys. Rev. Lett.* **90**, 167006 (2003).
- ³⁴M. Capone, M. Fabrizio, C. Castellani, and E. Tosatti, *Science* **28**, 2364 (2002).